Appearance of a two-dimensional antiferromagnetic order in quasi-one-dimensional cobalt oxides

J. Sugiyama,[1,*] H. Nozaki,[1] J. H. Brewer,[2] E. J. Ansaldo,[3] T. Takami,[4] H. Ikuta,[4] and U. Mizutani[4]
[1]*Toyota Central Research and Development Laboratories Inc., Nagakute, Aichi 480-1192, Japan*
[2]*TRIUMF, CIAR, and Department of Physics and Astronomy, University of British Columbia, Vancouver, British Columbia, Canada V6T 1Z1*
[3]*TRIUMF , 4004 Wesbrook Mall, Vancouver, British Columbia, Canada V6T 2A3*
[4]*Department of Crystalline Materials Science, Nagoya University, Furo-cho, Chikusa-ku, Nagoya, 464-8603 Japan*
(Received 18 December 2004; revised manuscript received 18 March 2005; published 10 August 2005)

By means of muon spin rotation and relaxation (μ^+SR) techniques, we have investigated the magnetism of quasi-one-dimensional (1D) cobalt oxides $A_{n+2}Co_{n+1}O_{3n+3}$ (A=Ca, Sr, and Ba; n=1, 2, 3, 5, and ∞), in which the 1D CoO_3 chain is surrounded by six equally spaced chains forming a triangular lattice in the *ab* plane, using polycrystalline samples, from room temperature down to 1.8 K. For the compounds with n=1–5, transverse field μ^+SR experiments showed the existence of a magnetic transition below ~100 K, although there were no clear anomalies in the susceptibility-vs-T curve. The onset temperature of the transition (T_c^{on}) was found to decrease with n; from 100 K for n=1 to 60 K for n=5. A damped muon spin oscillation was observed only in the sample with n=1 ($Ca_3Co_2O_6$), whereas only a fast relaxation obtained even at 1.8 K in the other three samples. Combining the fact that the paramagnetic Curie temperature ranges from −150 to −200 K for the compound with n=2 and 3, the μ^+SR result indicates that a two-dimensional (2D) short-range antiferromagnetic (AF) order, which has been thought to be unlikely to exist at high T due to a relatively strong 1D ferromagnetic (F) interaction, appears below T_c^{on} for all compounds with n=1–5; but quasistatic long-range AF order formed only in $Ca_3Co_2O_6$, below 25 K. For $BaCoO_3$ (n=∞), as T decreased from 300 K, 1D F order appeared below 53 K, and a sharp 2D AF transition occurred at 15 K.

DOI: 10.1103/PhysRevB.72.064418 PACS number(s): 76.75.+i, 75.40.Cx, 75.50.Ee

I. INTRODUCTION

In the two-dimensional (2D) layered cobalt oxides, Na_xCoO_2, $[Ca_2CoO_3]_{0.62}[CoO_2]$, and $[Ca_2Co_{4/3}Cu_{2/3}O_4]_{0.62}[CoO_2]$, a long-range magnetic order—which is clearly an incommensurate spin density wave in single crystalline samples—was previously found at low temperatures by positive muon spin rotation and relaxation (μ^+SR) experiments.[1–5] Several researchers reconfirmed later the existence of long-range magnetic order in Na_xCoO_2 by not only μ^+SR (Ref. 6) but also neutron diffraction experiments.[7] These cobaltites share a common structural component as a conduction path, i.e., the CoO_2 planes, in which a two-dimensional-triangular lattice of Co ions is formed by a network of edge-sharing CoO_6 octahedra.

This leads naturally to the question of the (cause and effect) interrelationship between magnetism and dimensionality. That is, what is the most stable spin configuration as a function of a spin density in low-dimensional systems? Recently, a homologous series of $A_{n+2}B'B_nO_{3n+3}$ (A=Ca, Sr, Ba, B' and B=Co) was discovered, in which charge carrier transport is restricted mainly to a one-dimensional (1D) $[B'B_nO_{3n+3}]$ chain.[8,9] Each chain is surrounded by six equally spaced chains forming a triangular lattice in the *ab* plane, as seen in Figs. 1 and 2. The $[B'BO_6]$ chain in the n=1 compound consists of alternating face-sharing $B'O_6$ trigonal prisms and BO_6 octahedra. As n increases, only the number of $[BO_6]$ octahedra increases so as to build the chain with n $[BO_6]$ octahedra and one $B'O_6$ trigonal prism (see Fig. 2).

The n=1 compound, $Ca_3Co_2O_6$, in particular, has attracted much attention for the past eight years,[10–16] because it is considered to be a typical quasi-1D system. It was found that $Ca_3Co_2O_6$ exhibits a transition from a paramagnetic to an antiferromagnetic state below 24 K (=T_N),[11] although the magnetic structure is not fully understood even after neutron scattering studies, probably due to the competition between the intrachain ferromagnetic (F) and interchain antiferromagnetic (AF) interactions.[11,12] The valence state of the Co ions was assigned to be +3; also, the spin configuration of Co^{3+} ions in the CoO_6 octahedron is the low-spin (LS) state with S=0 and in the CoO_6 prism the high-spin (HS) state with S=2.[11,17,18] At lower temperatures, magnetization and ^{59}Co-NMR measurements suggested the existence of a ferrimagnetic transition around 10 K,[12,13,19] which, however, was not seen in the specific heat (C_p).[20] Furthermore, the C_p measurement revealed an indication of either a short-range mag-

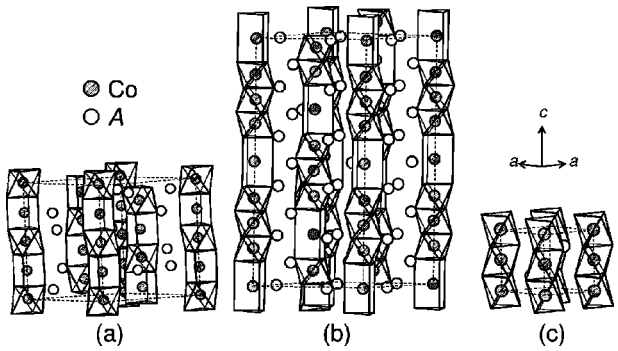

FIG. 1. Structures of the quasi-one-dimensional cobalt oxides $A_{n+2}B'B_nO_{3n+3}$ (A=Ca, Sr, Ba, B' and B=Co). (a) n=1, (b) n=3, and (c) n=∞.

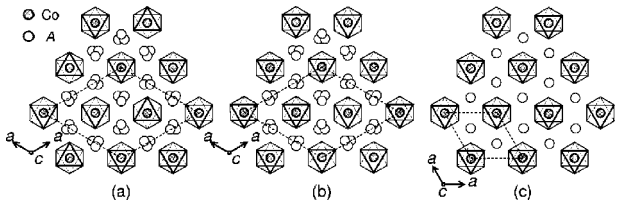

FIG. 2. *C*-plane view of $A_{n+2}B'B_nO_{3n+3}$ (A=Ca, Sr, Ba, B' and B=Co). (a) n=1, 2, and 3, (b) n=4 and 5, and (c) $n=\infty$.

netic order or a gradual change in the spin state of Co ions at higher temperatures (100–200 K).[20]

The other end member, $BaCoO_3$ ($n=\infty$), crystallizes in the hexagonal perovskite structure, in which the face-sharing CoO_6 octahedra form a 1D CoO_3 chain. The chains locate on a corner of the two-dimensional-triangular lattice separated by Ba ions.[21] Although a weak ferromagnetic, ferrimagnetic, or spin-glass-like behavior was observed below ~100 K in the susceptibility,[22,23] so far there are no reported studies using neutron scattering, NMR or μ^+SR on $BaCoO_3$. Additionally, a recent electronic structural calculation (LDA+U) predicted a ferromagnetic ground state as the most stable configuration.[24] The structure of $BaCoO_3$ is the same to that of $CsCoCl_3$ and/or $BaVS_3$,[25,26] which are known as typical 1D systems with $S=1/2$. The electronic configuration (t_{2g}^5) of Co^{4+} ions in $BaCoO_3$ suggests that the nature of $BaCoO_3$ is more like that of $BaVS_3$ (with t_{2g}^1 for V^{4+}) than that of $CsCoCl_3$ ($t_{2g}^5 e_g^2$ for Co^{2+}, but a fictitious spin $S'=1/2$ due to crystal field splitting).[27] In other words, the interaction between t_{2g} orbitals presumably plays the dominant role for magnetism in both $BaCoO_3$ and $BaVS_3$. Also, $BaVS_3$ exhibits a structural phase transition at 240 K, a metal-insulator transition at 69 K, and an AF transition at ~30 K.[28,29] However, a zero field (ZF) μ^+SR experiment on $BaVS_3$ did not detect muon spin oscillations, even at 2.2 K, but only a fluctuating random field well described by a dynamic Kubo-Toyabe relaxation function.[30]

For the compounds with $2 \leqslant n < \infty$, there are very limited data on physical properties, except for the structural data.[8,9] Very recently, Takami *et al.* reported transport and magnetic properties for the compounds with n=2–5.[31] According to their susceptibility (χ) measurements, there are no drastic changes in the $\chi(T)$ curve below 300 K for all these compounds, while the slope of χ^{-1} changes at ~180 K for the compounds with n=2 and 3.

As n increases from 1, the Co valence increases from +3 and approaches +4 with increasing n up to ∞, i.e., $BaCoO_3$. Also the ratio between prism and octahedron in the 1D CoO_3 chain reduces from 1/1 for n=1 to 0 for $n=\infty$.[9] Further systematic research on $A_{n+2}B'B_nO_{3n+3}$ is therefore needed to provide more significant information concerning the dilution effect of HS Co^{3+} in the 1D chain on magnetism. In particular, muon spin spectroscopy, as it is very sensitive to the local magnetic environment, is expected to yield crucial data in frustrated low-dimensional systems, as was the case for the 2D layered cobaltites.[1–5] This is because μ^+ only feels the magnetic fields due to its nearest neighbors and it is especially sensitive to short-range magnetic order, such as appeared in low-dimensional systems, whereas both neutron scattering and χ measurements mainly detect long-range magnetic order; for, if the correlation length is very short neutron diffraction peaks would broaden and eventually disappear.

TABLE I. Composition and lattice parameters for quasi-one-dimensional cobalt oxides, $A_{n+2}B'B_nO_{3n+3}$ (A=Ca, Sr, Ba, B' and B=Co). Here, $b=a$, $\alpha=\beta=90°$, and $\gamma=120°$.

n	Composition	a (Å)	Lattice Parameters c (Å)	Space group
1	$Ca_3Co_2O_6$	9.07	10.38	$R\bar{3}c$
2	$Sr_4Co_3O_9$	9.35	10.57	$P321$
3	$Sr_5Co_4O_{12}$	9.4	20.2	$P3c1$
5	$(Sr_{0.5}Ba_{0.5})_7Co_6O_{18}$	9.7	30.2	$P\bar{3}c1$
∞	$BaCoO_3$	5.65	4.75	$P6_3/mmc$

Here we report on a series of measurements at both weak (relative to the spontaneous internal fields in the ordered state) transverse field (wTF-)μ^+SR and (ZF-)μ^+SR for polycrystalline n=1, 2, 3, 5, and ∞ compounds at temperatures between 1.8 and 300 K. The former method is sensitive to local magnetic order *via* the shift of the μ^+ spin precession frequency in the applied field and the enhanced μ^+ spin relaxation, while ZF-μ^+SR is uniquely sensitive to weak local magnetic (dis)order in samples exhibiting quasistatic paramagnetic moments.

II. EXPERIMENT

Polycrystalline samples of quasi-1D cobalt oxides were synthesized at Nagoya University by a conventional solid-state reaction technique, using reagent grade Co_3O_4, $CaCO_3$, $SrCO_3$, and $BaCO_3$ powders as starting materials. For $BaCoO_3$, a sintered pellet was annealed at 650°C for 150 h in oxygen under pressure of 1 MPa. Powder x-ray diffraction (XRD) studies indicated that the samples were single-phase hexagonal structures. The composition and lattice parameters of the five samples are summarized in Table I. The preparation and characterization of the samples with n=1–5 were reported in detail elsewhere.[31]

Magnetic susceptibility (χ) was measured using a superconducting quantum interference device (SQUID) magnetometer (MPMS, Quantum Design) at temperatures between 2 and 600 K with magnetic field $H \leqslant 55$ kOe. Heat capacity (C_p) was measured using a relaxation technique (PPMS, Quantum Design) in the temperature range between 300 and 1.9 K. The μ^+SR experiments were performed on the M20 surface muon beam line at TRIUMF. The experimental setup and techniques were described elsewhere.[32]

III. RESULTS

A. n=1 compound, $Ca_3Co_2O_6$

The wTF-μ^+SR spectra in a magnetic field of $H \sim 90$ Oe in the $Ca_3Co_2O_6$ (n=1) sample, exhibit a clear reduction of the μ^+ precession amplitude below ~100 K. The wTF-μ^+SR spectrum below ~100 K was well fitted in the

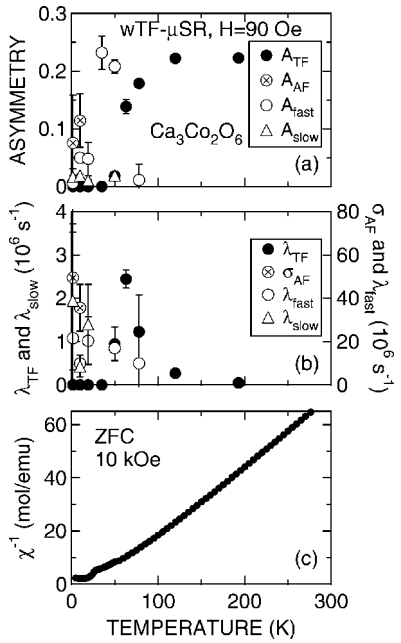

FIG. 3. Temperature dependences of (a) A_n and (b) λ_n and σ_{AF}, and (c) inverse susceptibility χ^{-1} in $Ca_3Co_2O_6$ ($n=1$). The data were obtained by fitting the wTF-μ^+SR spectra using Eq. (1). χ was measured with the magnetic field $H=10$ kOe in the zero-field cooling mode (Ref. 31).

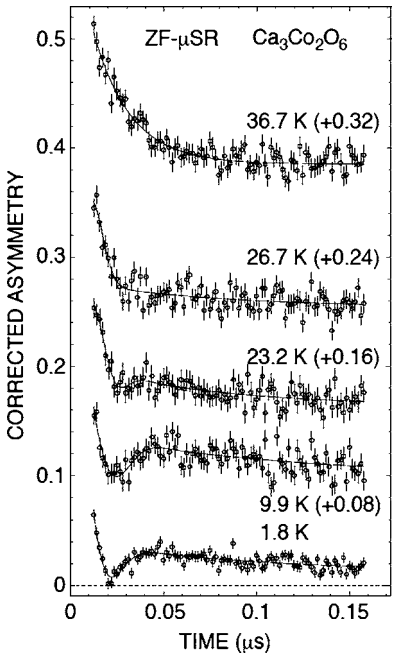

FIG. 4. ZF-μ^+SR spectra for $Ca_3Co_2O_6$ at 1.8, 9.9, 23.2, 26.7, and 36.7 K. The spectra are each shifted upward by 0.08 for clarity of the display.

time domain with a combination of four signals; a slowly relaxing precessing signal from muons in the paramagnetic fraction of the sample, a fast Gaussian relaxing precessing signal from muons experiencing quasistatic internal fields below the transition temperature, plus two minor background signals: a slow and a fast nonoscillatory background signal attributed to regions with high- and/or fast-fluctuating fields, namely,

$$A_0P(t) = A_{TF}\exp(-\lambda_{TF}t)\cos(\omega_{\mu,TF}t + \phi_{TF}) + A_{AF}\exp(-\sigma_{AF}{}^2t^2)\cos(\omega_{\mu,AF}t + \phi_{AF}) + A_{fast}\exp(-\lambda_{fast}t) + A_{slow}\exp(-\lambda_{slow}t), \quad (1)$$

where A_0 is the initial ($t=0$) asymmetry, $P(t)$ is the muon spin polarization function, $\omega_{\mu,TF}$ and $\omega_{\mu,AF}$ are the muon Larmor frequencies corresponding to the applied weak transverse field and the internal antiferromagnetic field, ϕ_{TF} and ϕ_{AF} are the initial phases of the two precessing signals, A_n and λ_n (n=TF, fast, and slow) are the asymmetries and exponential relaxation rates of the three signals, and A_{AF} and σ_{AF} are the asymmetry and Gaussian relaxation rate of the AF signal. The fast Gaussian relaxing precessing signal has a finite amplitude below ~30 K and the two nonoscillatory signals (n=fast and slow) below ~80 K.

Figures 3(a)–3(c) show the temperature dependences of A_n (n=TF, AF, fast, and slow), λ_{TF}, σ_{AF}, λ_{fast}, λ_{slow}, and inverse susceptibility χ^{-1} measured in field cooling mode with $H=10$ kOe in the $Ca_3Co_2O_6$ sample ($n=1$ compound). As T decreases from 200 K, the magnitude of A_{TF} is nearly independent of temperature down to 100 K; then A_{TF} decreases rapidly as T is lowered further.[33] Finally A_{TF} levels off to zero at temperatures below ~30 K. This indicates the existence of a magnetic transition below ~100 K. Since A_{TF} is proportional to the volume of a paramagnetic phase, the volume fraction V_F of the magnetic phase below 30 K is estimated to be ~ 100%. On the other hand, the $A_{fast}(T)$ curve exhibits a maximum at ~30 K, probably due to the onset of even stronger local fields (resulting in unobservably fast muon spin depolarization) below 30 K. The magnitude of A_{fast} reaches the full asymmetry of ~0.22 at the maximum. The two other signals, A_{AF} and A_{slow}, appear below ~20 K, whereas A_{fast} seems to disappear below 20 K.

Both the $\lambda_{TF}(T)$ and the $\lambda_{fast}(T)$ curves exhibit a broad maximum ~60 K and 30 K, respectively. That is, λ_{TF} increases with decreasing T from 200 K to 60 K, then decreases below 60 K. Meanwhile, λ_{fast} increases with decreasing T from ~80 K (where it is first detected) down to 30 K, after which it decreases down to the lowest temperature measured. It is noteworthy that the highest value of $\lambda_{fast}(\sim 60\times10^6\ s^{-1})$ is 20 times larger than that of $\lambda_{TF}(\sim 3\times10^6\ s^{-1})$.

In order to elucidate magnetism below 30 K in greater detail, Fig. 4 shows ZF-μ^+SR time spectra for $Ca_3Co_2O_6$ below 36.7 K. The spectrum at 36.7 K consists mainly of a fast relaxed nonoscillatory signal, while below 23.2 K a first minimum and maximum are clearly seen, indicative of a fast relaxing oscillation. Indeed, this spectrum is reasonably well fitted with a combination of a Gaussian relaxing cosine oscillation (for a quasistatic internal field) and fast and slow exponential relaxation functions (for fluctuating moments), given by the last three terms in Eq. (1). Moreover, it was very difficult to fit using Kubo-Toyabe functions, which describe a random field distribution. We therefore conclude that $Ca_3Co_2O_6$ undergoes a magnetic transition to a long-range

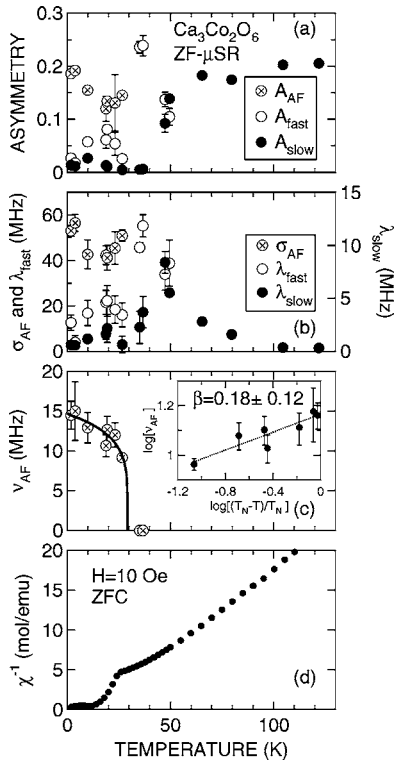

FIG. 5. Temperature dependences of (a) A_n, (b) σ_{AF}, and λ_n, (c) muon precession frequency $\nu_{AF}2\pi=\omega_{\mu,AF}$, and (d) χ^{-1} measured in a zero-field cooling mode with $H=10$ Oe (Ref. 31) in $Ca_3Co_2O_6$. The data were obtained by fitting the ZF-μ^+SR spectra using the latter three terms in Eq. (1). The solid line in Fig. 5(c) represents the fitting curve using Eq. (2). The inset of Fig. 5(c) shows the log-log plot of ν_{AF} as a function of reduced temperature.

ordered state below ~30 K. Only the first minimum and maximum can be observed in the spectra even at 1.8 K, indicating that the formation of the long-range order is strongly suppressed probably due to geometrical frustration in the triangular lattice. Actually, a partially disordered antiferromagnetic (PDA) state, in which two-thirds of the chains exhibit AF order, but the remaining one-third remains incoherent, is proposed for $Ca_3Co_2O_6$ below T_N. A spin freezing behavior was also observed below 10 K.[12] Such a PDA and/or spin freezing state is consistent with oscillatory signals strongly damped by field inhomogeneity.

Figures 5(a)–5(d) show the temperature dependences of A_n (n=AF, fast, and slow), σ_{AF}, λ_{fast}, λ_{slow}, and muon precession frequency $\nu_{AF}(=\omega_{\mu,AF}/2\pi)$ in $Ca_3Co_2O_6$. The oscillating signal has a finite intensity below 27 K, while the slow exponential relaxed signal disappears below ~30 K. This means that the magnetic moment fluctuating at high temperatures slows down with decreasing T and then orders below 27 K, and becomes quasistatic (within the experimental time scale). The T dependence of ν_{AF}, which is an order parameter of the transition, is in good agreement with the T dependence of the intensity of the AF magnetic diffraction peak determined by a neutron experiment.[11] Actually, the $\nu_{AF}(T)$ curve is well fitted by the following expression:

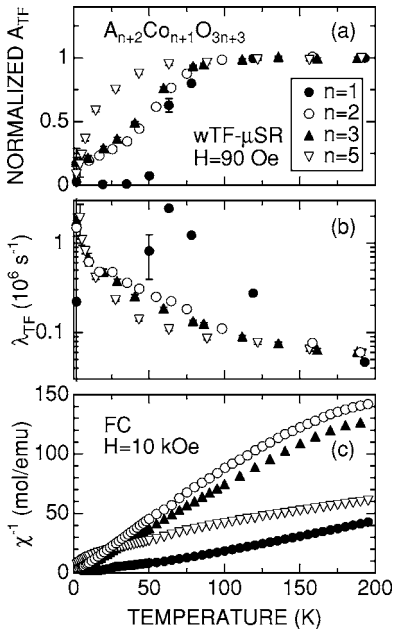

FIG. 6. Temperature dependences of (a) normalized A_{TF}, (b) λ_{TF}, and (c) inverse susceptibility χ^{-1} in $Ca_3Co_2O_6$ ($n=1$), $Sr_4Co_3O_9$ ($n=2$), $Sr_5Co_4O_{12}$ ($n=3$), and $(Ba_{0.5}Sr_{0.5})_7Co_6O_{18}$ ($n=5$). χ was measured with magnetic field $H=10$ kOe in field cooling mode (Ref. 31).

$$\nu_{AF}(T) = \nu_{AF}(0\ \mathrm{K}) \times \left(\frac{T_N - T}{T_N}\right)^{\beta}. \quad (2)$$

This provides $\nu_{AF}(0\mathrm{K})=14.6\pm0.8$ MHz, $\beta=0.18\pm0.12$, and $T_N=29\pm5$ K [see Fig. 5(c)]. In spite of the low accuracy of the fitting (and over a wide range of T), the exponent (β) obtained lies between the predictions (of the critical exponent values) for the 2D and 3D Ising models ($\beta=0.125$ and 0.3125),[34] although we need more accurate data in the vicinity of T_N to determine β more precisely and relate it more conclusively to the dimensionality of the transition. The value of T_N is also in good agreement with the results of χ and neutron diffraction measurements ($T_N=24$ K).[11] These results confirm that muons experience the internal magnetic field due to the long-range 2D AF order. It should be noted that there are no marked anomalies in the ZF-μ^+SR results around 10 K corresponding to the ferrimagnetic transition temperature.[12] This is very reasonable because the ferrimagnetism is induced by the external field.

Longitudinal-field (LF-)μ^+SR measurements, which we do not report here in detail, are most useful in cases where the ZF-spectrum is explained by Kubo-Toyabe functions, because the applied LF competes with the internal random field distribution and aligns the muon spins in its original direction. As a result, we can distinguish whether the field distribution is static or dynamic.[32] On the other hand, the ZF-spectrum for $Ca_3Co_2O_6$ is well fitted by the damped cosine oscillation due to the static magnetic field with $\nu_{AF}(0\ \mathrm{K})\sim14.6$ MHz. The magnitude of A_{AF} is ~0.2 at 1.8 K, indicating the static magnetic ordered phase is predominant in $Ca_3Co_2O_6$. Since the result is consistent with those of

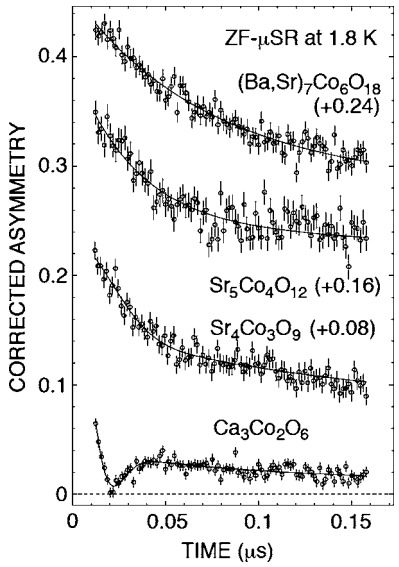

FIG. 7. ZF-μ^+SR spectra at 1.8 K for $Ca_3Co_2O_6$ ($n=1$), $Sr_4Co_3O_9$ ($n=2$), $Sr_5Co_4O_{12}$ ($n=3$), and $(Ba_{0.5}Sr_{0.5})_7Co_6O_{18}$ ($n=5$). The spectra are each shifted upward by 0.08 for clarity of the display.

the χ and neutron diffraction measurements, which detect the static long-range magnetic order, we conclude that the internal magnetic field is static. Indeed, our preliminary LF-μ^+SR measurement at 1.8 K also supported this conclusion.

There are two probable explanations for the decrease in A_{TF} below 100 K. One is a conventional scenario, in which a short-range 1D F order appears below 100 K as proposed by Aasland *et al.*[11] and probably completes below ~40 K, because both A_{TF} (Fig. 3) and A_{slow} (Fig. 5) seem to level off to their minimum value (~0) below ~40 K. The long-range 2D AF order then appears below 27 K. The other scenario is more ambitious; that is, a short-range 2D AF order appears below 100 K and completes below 27 K. This means that the 1D F order should exist above 100 K, which is not supported by the present μ^+SR experiments. Based only on the result in $Ca_3Co_2O_6$, it is difficult to determine which scenario is more probable. We will therefore discuss this problem later.

B. n=2, 3 and 5 compounds

Figures 6(a)–6(c) show the temperature dependences of (a) normalized $A_{TF}(N_{A_{TF}})$, (b) λ_{TF}, and (c) χ^{-1} in $Ca_3Co_2O_6$ ($n=1$), $Sr_4Co_3O_9$ ($n=2$), $Sr_5Co_4O_{12}$ ($n=3$), and $(Ba_{0.5}Sr_{0.5})_7Co_6O_{18}$ ($n=5$).

The data were obtained by fitting the wTF-μ^+SR spectra using Eq. (1) without the oscillatory signal due to a static internal antiferromagnetic magnetic field (the A_{AF} signal). In order to compare the value of A_{TF} for these samples, $N_{A_{TF}}$ is defined as

$$N_{A_{TF}} = \frac{A_{TF}(T)}{A_{TF,max}}, \tag{3}$$

in which $A_{TF,max}$ is the maximum value of A_{TF}. Since $A_{TF,max}$ corresponds to A_{TF} for the paramagnetic state, $N_{A_{TF}}$ is roughly equivalent to the volume fraction of the paramagnetic phase in the sample.

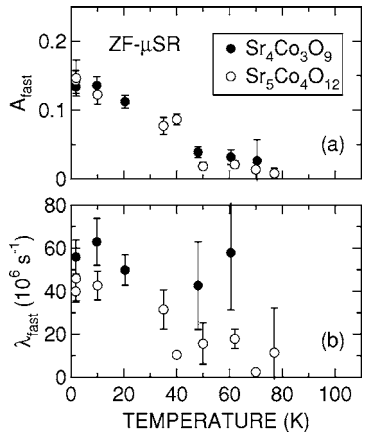

FIG. 8. Temperature dependences of (a) asymmetry A_{fast} and (b) relaxation rate λ_{fast} of a fast exponential relaxation signal for $Sr_4Co_3O_9$ ($n=2$) and $Sr_5Co_4O_{12}$ ($n=3$). The data were obtained by fitting the ZF-μ^+SR spectrum using Eq. (4).

All four samples show the magnetic transition below 100 K; the onset temperatures of the transition (T_c^{on}) are estimated as 100±25 K for $n=1$, 90±10 K for $n=2$, 85±10 K for $n=3$, and 50±10 K for $n=5$, respectively. The magnitude of T_c^{on} is thus found to decrease with n. It should be noted that there are no marked anomalies in the $\chi^{-1}(T)$ curve measured with $H=10$ kOe at T_c^{on} for the four compounds. Although $N_{A_{TF}}$ for the $n=1$ compound levels off to its minimum value (~0) below 30 K, the $N_{A_{TF}}(T)$ curve for the other three compounds never reaches their minimum even at 1.8 K, indicating that the internal magnetic field is still fluctuating. Indeed, λ_{TF} for the samples with $n=2$, 3, and 5 increases monotonically with decreasing T, whereas the $\lambda_{TF}(T)$ curve for $Ca_3Co_2O_6$ ($n=1$) exhibits a sharp maximum around 55 K.

In spite of the large decrease in A_{TF} below 100 K for the samples with $n=2$, 3, and 5, the ZF-μ^+SR spectra exhibit no oscillations even at 1.8 K as seen in Fig. 7. This indicates that the magnetic moment appears below T_c^{on}, but is still fluctuating at 1.8 K. The ZF-μ^+SR spectra are well fitted by a combination of fast and slow exponential relaxation functions (for fluctuating moments) and a dynamical Kubo-Toyabe function G^{DGKT} (for a fluctuating random moment component)

$$A_0P(t) = A_{fast}\exp(-\lambda_{fast}t) + A_{slow}\exp(-\lambda_{slow}t) + A_{KT}\exp(-\lambda_{KT}t)G^{DGKT}. \tag{4}$$

In Fig. 8, the fast exponentially relaxed signal, which corresponds to the initial decay of the ZF-spectrum in Fig. 7, appears below ~80 K for the samples with $n=2$ and 3. The $A_{fast}(T)$ and $\lambda_{fast}(T)$ curves increase monotonically with decreasing T, as expected from the wTF-μ^+SR measurement. The magnitude of A_{fast} increases up to ~0.14 at 1.8 K, whereas $A_{slow}\sim 0.07$ and $A_{KT}\sim 0.04$. The fast exponentially

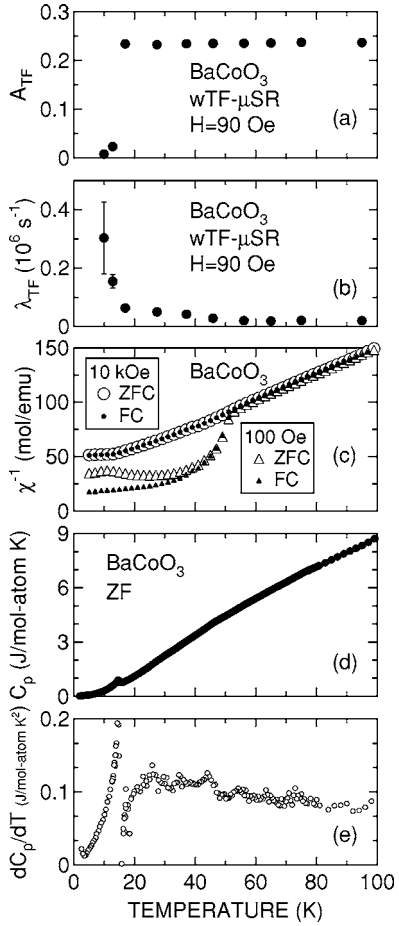

FIG. 9. Temperature dependences of (a) weak transverse field asymmetry A_{TF}, (b) exponential relaxation rate λ_{TF}, (c) inverse susceptibility χ^{-1}, (d) specific heat C_p, and (e) its temperature derivative dC_p/dT for $BaCoO_3$ ($n=\infty$). A_{TF} and λ_{TF} were obtained by fitting the wTF-μ^+SR spectra with $A_{TF}\exp(-\lambda_{TF}t)\cos(\omega_{\mu,TF}t+\phi_{TF})$. χ was measured with magnetic field $H=10$ kOe and 100 Oe in both zero-field cooling (ZFC) and field cooling (FC) mode.

relaxed signal is therefore predominant in the ZF-μ^+SR spectra for both compounds. The fitted values of λ_{fast} at the lowest T(=1.8 K) were 55×10^6 s^{-1} for $Sr_4Co_3O_9$ ($n=2$), 40×10^6 s^{-1} for $Sr_5Co_4O_{12}$ ($n=3$), and 18×10^6 s^{-1} for $(Ba_{0.5}Sr_{0.5})_7Co_6O_{18}$ ($n=5$). Since these are comparable to the value of σ_{AF}(1.8 K)(=55×10^6 s^{-1}) for $Ca_3Co_2O_6$, the fast exponentially relaxed signal in the samples with $n>1$ is most likely caused by an interchain 2D AF interaction. It should be noted that σ_{AF}(1.8 K) or λ_{fast}(1.8 K) decreases with n, suggesting that the magnitude of the 2D AF interaction is weakened with increasing n.

The number of oxygen sites in the lattice (z_O) depends on n; that is, $z_O=1$, 9, 12, 9, and 1 for $n=1$, 2, 3, 5, and ∞, respectively, indicating multiple μ^+ sites in the compounds with $n=2$–5. This is because, based on the huge number of μ^+SR works on cuprates, μ^+ sits about 1 Å away from an oxygen ion,[32] and there is no room for μ^+ in or very near the CoO_3 chains. The third term in Eq. (4), $A_{KT}\exp(-\lambda_{KT}t)G^{DGKT}$, is hence most likely to correspond to the signal from the μ^+s sitting on the multiple sites.

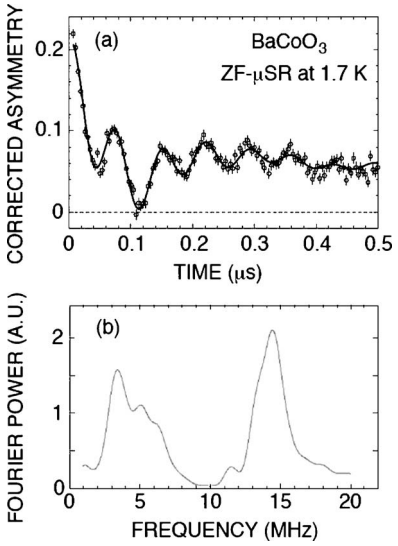

FIG. 10. (a) ZF-μ^+SR spectrum for $BaCoO_3$ ($n=\infty$) at 1.7 K and (b) Fourier transform of (a). The solid line in Fig. 8 represents the result of fitting using Eq. (5). The Fourier spectrum consists of five major components (with 14.4, 13.5, 6.4, 5.1, and 3.5 MHz) and probably three minor components (with 18, 11.5, and 1 MHz).

C. $n=\infty$ compound, $BaCoO_3$

Figures 9(a)–9(c) show the temperature dependences of (a) A_{TF}, (b) λ_{TF}, (c) χ^{-1}, (d) specific heat C_p, and (e) its temperature derivative dC_p/dT for $BaCoO_3$ ($n=\infty$). Both A_{TF} and λ_{TF} were obtained by fitting the wTF-μ^+SR spectra, the same way as the compounds with $n=2$–5. The $\chi^{-1}(T)$ curve indicates the existence of an AF transition at 14 K(=T_N) with $H=10$ kOe, but a weak F or ferrimagnetic behavior below 53 K with $H=100$ Oe. Also, the $C_p(T)$ curve shows a sharp maximum at 15 K, indicating the existence of a magnetic transition. However, at around 53 K, there are no clear anomalies in the $C_p(T)$ curve, although the slope (dC_p/dT) increases slightly around 50 K with decreasing T. The lack of a clear anomaly around 50 K in the $C_p(T)$ curve suggests that the transition at 53 K is induced by the 1D F order, as is the case for the 1D F order in $Ca_3Co_2O_6$.

The wTF-μ^+SR experiment with 90 Oe shows that, as T decreases from 100 K, A_{TF} drops suddenly down to ~0 at T_N, indicating that the whole sample enters into an AF state. Such abrupt change in A_{TF} is very different from those for the other quasi-1D cobalt oxides with $n=1$–5, which typically show a large transition width of 50 to 80 K. On the other hand, the $\lambda_{TF}(T)$ curve exhibits a small increase below $\sim$50 K with decreasing T, probably associated with the complicated magnetism observed in χ with low magnetic fields. As T decreases further from 50 K, λ_{TF} increases rapidly below 17 K, showing typical critical behavior toward T_N.

The ZF-μ^+SR spectrum at 1.7 K exhibits a clear but complex muon spin oscillation, displayed in Fig. 10(a). The Fourier transform of the ZF-μ^+SR time spectrum [Fig. 10(b)] indicates that the ZF-μ^+SR spectrum has *at least* five frequency components ($\nu_\mu=14.4$, 13.5, 6.4, 5.1, and 3.5 MHz), even though the sample is structurally a single phase at room temperature and there is no indication of any structural phase

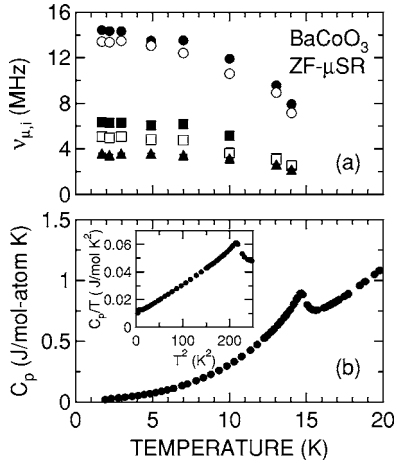

FIG. 11. Temperature dependences of (a) $\nu_{\mu,i}$ and (b) C_p for $BaCoO_3$ ($n=\infty$). The data of $\nu_{\mu,i}$ were obtained by fitting the ZF-spectrum with Eq. (5). The inset of (b) shows the dependence of C_p/T on T^2. Since C_p/T decreases roughly in proportion to T^2 below T_N^2, the magnetic contribution should not be ignored even at the lowest T measured. This means that it is extremely difficult to determine the Debye temperature and/or subtract the lattice contribution from the experimental data.

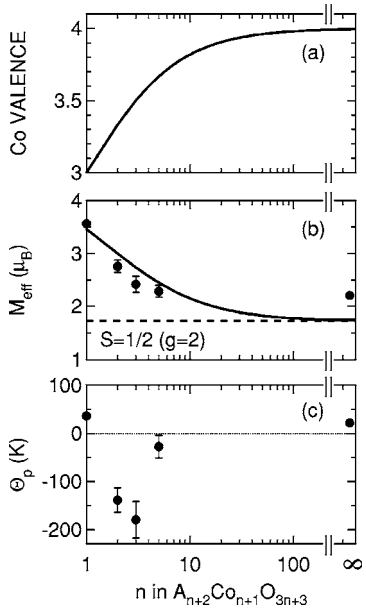

FIG. 12. (a) Average Co valence, (b) effective magnetic moment of Co ions (M_{eff}), and (c) paramagnetic Curie temperature (Θ_p) as a function of n in the 1D system, $A_{n+2}Co_{n+1}O_{3n+3}$.

transition down to 77 K in resistivity (ρ) and thermopower (TEP) measurements;[22] nor are there any anomalies in the $\chi(T)$ curve down to 4 K, except around T_N. This implies that there is presumably only one μ^+ site in the $BaCoO_3$ lattice, because every oxygen is equivalent for the simple hexagonal lattice ($z_O=1$). The ZF-spectra were well fitted by the following equation:

$$A_0P(t) = \sum_{i=1}^{5} A_{AF,i}\exp(-\lambda_{AF,i}t)\cos(\omega_{\mu,i}t+\phi) + \sum_{i=1}^{2} A_i\exp(-\lambda_i t), \quad (5)$$

where A_0 is the empirical maximum experimental muon decay asymmetry, $A_{AF,i}$ and $\lambda_{AF,i}$ ($i=1$–5) are the asymmetries and exponential relaxation rates associated with the five oscillating signals, and A_i and λ_i ($i=1$ and 2) are the asymmetries and exponential relaxation rates of the two nonoscillating signals as in Eqs. (1) and (4) (for the muon sites experiencing fluctuating magnetic fields).

The internal magnetic fields of the five signals, i.e., $\nu_{\mu,i}$ with $i=1$–5, exhibit a similar temperature dependence, as seen in Fig. 11(a). That is, as T decreases from 20 K, each $\nu_{\mu,i}$ suddenly appears below 15 K, at which the $C_p(T)$ curve shows a typical behavior for the AF transition [Fig. 11(b)], and increases with a decreasing slope $d\nu_{\mu,i}/dT$, then levels off to a constant value below 5 K. Here, it is worth noting that the $\nu_{\mu,i}$-vs-T curve indicates the change in an order parameter of the transition. Thus, the rapid temperature dependence of $\nu_{\mu,i}$ just below T_N suggests that the transition is likely to be continuous. Actually, the $C_p(T)$ curve also supports that the transition at 15 K is continuous. The five frequencies are therefore unlikely to be caused by compositional inhomogeneities, but most likely reflect the intrinsic behavior of $BaCoO_3$.

Although we ignored the contribution from the three minor oscillating signals, the relative fraction of the five signals is estimated as ~66% at 1.8 K which is typical for isotropic polycrystalline samples. This is because one-third of the fields oriented parallel to the initial muon spin direction (S_μ) due to randomly bound grains and/or domain structures do not result in precession, while the other two-thirds of the fields oriented perpendicular to S_μ cause precession. In other words, the minor signals correspond to less than ~1% of the volume of the sample.

IV. DISCUSSION

A. T_c^{on} for the compounds with $n=1$–5

In order to understand the common features of the macroscopic magnetism of the quasi-1D compounds taken collectively, Fig. 12 shows the average valence of Co (V_{Co}) ions, the effective magnetic moment of Co ions (M_{eff}) and the paramagnetic Curie temperature (Θ_p) as a function of n. The $V_{Co}(n)$ curve is calculated from the nominal composition of the 1D system; that is, we ignored a possible oxygen deficiency in the samples. The values of M_{eff} and Θ_p were obtained by fitting the $\chi(T)$ curve between 300 and 600 K using the Curie-Weiss law. The solid line in Fig. 12(b) represents the $M_{eff}(n)$ curve for the charge and spin distribution on the CoO_3 chain in Table II; that is, one Co^{3+} in the CoO_6 prism (Co^{3+}_{pri}) with the HS state ($S=2$) and one Co^{3+} and $(n-1)Co^{4+}$ in the CoO_6 octahedra (Co^{3+}_{oct} and Co^{4+}_{oct}) with the LS state ($S=0$ and 1/2). The relationship between M_{eff} and n is given by[35]

TABLE II. Composition and nominal charge and spin distribution in the CoO_3 chain for quasi-one-dimensional cobalt oxides, $A_{n+2}Co_{n+1}O_{3n+3}$ (A=Ca, Sr, Ba). Here, Co_{pri} and Co_{oct} denote the Co ion in a CoO_6 prism and in a CoO_6 octahedron. For the compounds with n=2–5, mixed valence state would exist in the neighboring CoO_6 octahedra to minimize electronic repulsion.

n	Composition	Charge distribution	Spin distribution
1	$Ca_3Co_2O_6$	$Co^{3+}_{pri}, Co^{3+}_{oct}$	2, 0
2	$Sr_4Co_3O_9$	$Co^{3+}_{pri}, Co^{3+}_{oct}, Co^{4+}_{oct}$	2, 0, 1/2
3	$Sr_5Co_4O_{12}$	$Co^{3+}_{pri}, Co^{3+}_{oct}, Co^{4+}_{oct}, Co^{4+}_{oct}$	2, 0, 1/2, 1/2
5	$(Sr_{0.5}Ba_{0.5})_7Co_6O_{18}$	$Co^{3+}_{pri}, Co^{3+}_{oct}, Co^{4+}_{oct}, Co^{4+}_{oct}, Co^{4+}_{oct}, Co^{4+}_{oct}$	2, 0, 1/2, 1/2, 1/2, 1/2
∞	$BaCoO_3$	Co^{4+}_{oct}	1/2

$$M^2_{\mathrm{eff}} = \left(\frac{1}{n+1} M^2_{\mathrm{eff,S=2}} + \frac{n-1}{n+1} M^2_{\mathrm{eff,S=1/2}} \right), \tag{6}$$

$$T_{\mathrm{N}} = \frac{1}{2} 2z |J_{\mathrm{AF}}| \frac{S(S+1)}{3k_{\mathrm{B}}}, \tag{7}$$

where $M_{\mathrm{eff,S=2}}$ and $M_{\mathrm{eff,S=1/2}}$ are M_{eff} for Co ions with S=2 and S=1/2 (Co^{3+}_{pri} and Co^{4+}_{oct}). Since the variation of measured M_{eff} below n=5 is well explained by Eq. (6), the above spin and charge configuration in the CoO_3 chain is the most probable one. This also suggests that the oxygen deficiency in the samples with $n \leqslant 5$ is very small. For $BaCoO_3$ (n=∞), M_{eff} is estimated as 2.2 μ_{B}, whereas it is M_{eff}=1.73 μ_{B} for Co^{4+}_{oct} with S=1/2. This discrepancy was also reported by another group ($M_{\mathrm{eff}} \sim 2.3\ \mu_{\mathrm{B}}$) and was explained using a large g factor (=2.2) for the Co ions,[22] although g=2.0 for Fe-doped $Ca_3Co_2O_6$ was found in an electron spin resonance study.[36]

For $Ca_3Co_2O_6$ (n=1), Θ_{p}=36.1±0.8 K, and this is consistent with past work.[12,13] As n increases from 1 to 3, Θ_{p} changes its sign from positive to negative and rapidly decreases down to −180 K, then increases with further increasing n and approaches 22 K at n=∞. A large negative paramagnetic Curie temperature for the samples with n=2 and 3 obviously indicates that the transition at $T^{\mathrm{on}}_{\mathrm{c}}$ is caused by an interchain 2D AF interaction. Considering the structural similarity among the quasi-1D cobalt oxides, $T^{\mathrm{on}}_{\mathrm{c}}$ for the samples with n=1 and 5 are therefore most likely due to the appearance of the short-range 2D AF order. The magnitude of the 1D F interaction would be strongly affected by n, because not only the structure of the chain but also the Co valence are altered by n (see Table II). Compared with the the intrachain 1D F interaction, the interchain 2D AF interaction is expected to be insensitive to n, as the geometrical arrangement of the chains in the ab plane is essentially the same for all the compounds with n=1–∞. This indicates that the interchain AF interaction plays a significant role for determining the magnetism detected by the current μ^+SR measurements. Here we wish to emphasize that $T^{\mathrm{on}}_{\mathrm{c}}$ is not caused by the change in the spin state of Co ions proposed by Hardy *et al.*,[20] because the decrease in A_{TF} confirms the appearance of a magnetically ordered phase. On the contrary, it was found that not A_{TF} but λ_{TF} exhibit an anomaly at the spin state transition in the layered cobaltites.[3]

Since each chain is considered to act as a single spin, we ignore the intrachain 1D F interaction. Within the mean field theory, T_{N} is expressed by

where z is the number of the nearest-neighbor spins, J_{AF} is the 2D AF coupling constant, and k_{B} is the Boltzmann constant. Although T_{N}=29±5 K for $Ca_3Co_2O_6$ from the ZF-μ^+SR measurement, we introduce a virtual $T_{\mathrm{N}}(T'_{\mathrm{N}})$ to explain the behavior of the $A_{\mathrm{TF}}(T)$ curve, indicating the appearance of the short-range 2D AF order. Assuming that $T^{\mathrm{on}}_{\mathrm{c}}$ (or $T^{\mathrm{mid}}_{\mathrm{c}}$) $=T'_{\mathrm{N}}$ and z=6, we can estimate J_{AF} for the current samples using the spin distribution in Table II. Here, $T^{\mathrm{mid}}_{\mathrm{c}}$ denotes the temperature at which $N_{A_{\mathrm{TF}}}$=0.5.

Figures 13(a) and 13(b) show the variation of T_{c} and J_{AF} as a function of the interchain distance $d_{\mathrm{interchain}}$ in $A_{n+2}Co_{n+1}O_{3n+3}$. Although T_{c} decreases with $d_{\mathrm{interchain}}$ (and/or n), the magnitude of $J_{\mathrm{AF}}/k_{\mathrm{B}}$ is roughly the same (∼20 K or 10 K) for all the samples. This suggests that $T^{\mathrm{on}}_{\mathrm{c}}$ is induced by the 2D AF interaction not only for the compounds with $n \geqslant 2$, but also for $Ca_3Co_2O_6$.

For $BaCoO_3$, the lowest $T^{\mathrm{on}}_{\mathrm{c}}$ and the sharp transition width are characteristic features compared with those for the com-

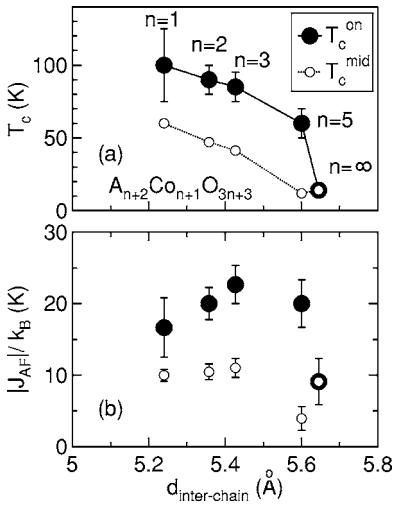

FIG. 13. The relationship between the interchain distance $d_{\mathrm{interchain}}$ and (a) T_{c} and (b) J_{AF} in the quasi-1D system, $A_{n+2}Co_{n+1}O_{3n+3}$. The solid and open circles in (a) represent $T^{\mathrm{on}}_{\mathrm{c}}$ and $T^{\mathrm{mid}}_{\mathrm{c}}$ and those in (b) corresponding J_{AF}; $T^{\mathrm{mid}}_{\mathrm{c}}$ is defined as the temperature at which $N_{A_{\mathrm{TF}}}$=0.5.

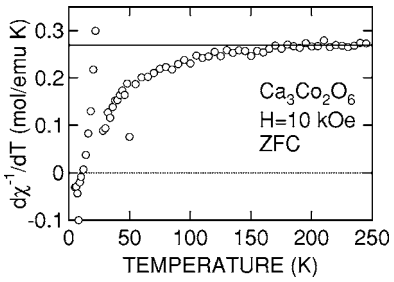

FIG. 14. Temperature dependence of the slope of χ^{-1} ($d\chi^{-1}/dT$) for $Ca_3Co_2O_6$. χ are the data shown in Fig. 3(c).

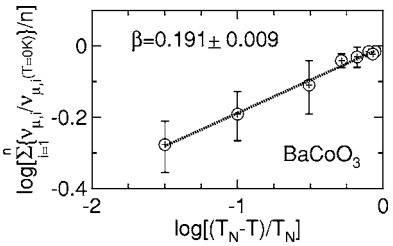

FIG. 15. Log-log plot of the average of normalized oscillation frequencies as a function of reduced temperature for $BaCoO_3$.

pounds with $n \leqslant 5$ (see Figs. 6 and 9). Also, a clear muon oscillation is observed only in $BaCoO_3$ below 15 K. These suggest a smaller fluctuation and/or distribution of the internal magnetic field in $BaCoO_3$ than in the compounds with $n \leqslant 5$. As seen in Table II, Co^{4+} ions with $S=1/2$ (Co^{4+}_{oct}) are stable in $BaCoO_3$, while both Co^{3+} ions with $S=2$ and $S=0$ (Co^{3+}_{pri} and Co^{3+}_{oct}) coexist in $Ca_3Co_2O_6$ and Co^{3+}_{pri},Co^{3+}_{oct}, and Co^{4+}_{oct} in the compounds with $n=2$–5. A mixed valence state is expected in the neighboring Co^{3+}_{oct} and Co^{4+}_{oct} ions for minimizing electronic repulsion, indicating the existence of a fluctuating magnetic field. Also, the spin and charge distribution in the compounds with $n \leqslant 5$ would induce a large distribution in the internal magnetic field. These are most likely to be the reasons for the difference between $BaCoO_3$ and the compounds with $n \leqslant 5$.

B. Ferromagnetic order along the chain

As seen in Fig. 9, the $\chi^{-1}(T)$ curve for $BaCoO_3$ exhibits a weak F or ferrimagnetic behavior below 53 K only under low magnetic fields. Reflecting this change, λ_{TF} increases slightly below ~50 K with decreasing T, while there are no anomalies in the A_{TF} curve down to 15 K. It is therefore most reasonable to conclude that, as T decreases, the 1D F order completes below 53 K, then the 2D AF order becomes stable below 15 K. In other words, the F order in the chain is easily observed by χ measurements but looks very complex in μ^+SR. This situation is similar to the case for the typical 1D antiferromagnet $CsCoCl_3$, in which the short-range 1D AF order appears below 75 K.[27] This corresponds to the maximum in the $\chi(T)$ curve. Nevertheless, moving solitons along the chain[37] induce a large fluctuation of the internal field at the muon sites. As a result, μ^+SR was able to detect the 2D AF order but unable to observe the short-range 1D AF order.[38]

For the compounds with $n=1$–5, we propose that T_c^{on} (or T_c^{mid})$=T'_N$ is caused by the 2D AF interaction. Hence, there should exist a transition into the short-range 1D F ordered state above T_c^{on}. For $Ca_3Co_2O_6$, this requirement is very consistent with the indication of a short-range magnetic order below ~200 K detected by a specific heat measurement.[20] The $\chi^{-1}(T)$ curve for the current $Ca_3Co_2O_6$ also exhibits a deviation from the linear relationship below ~ 150 K (see Fig. 14),[13] presumably indicating the appearance of the 1D F order.

Furthermore, recent χ measurements for the compounds with $n=2$–5 showed a field dependence even at 300 K.[39] This may be due to the appearance of short-range 1D F order along the chain. The overall scenario for the quasi-1D systems is therefore that the 1D F ordered state exists even at ~200 K, while the 2D AF ordered state appears below ~100 K. The former is very difficult to detect by μ^+SR and neutron diffraction measurements, but the latter can be relatively easily observed by μ^+SR.

C. Multifrequency components in $BaCoO_3$

In order to evaluate the critical exponent (β) for the AF transition, Fig. 15 shows the relationship between the normalized oscillation frequency $\nu_{\mu,i}/\nu_{\mu,i}(0K)$ and the reduced temperature $(T_N-T)/T_N$. Here, $\nu_{\mu,i}(0K)$ and T_N are obtained by fitting the $\nu_{\mu,i}(T)$ curve (Fig. 11) with Eq. (2). We obtain $\beta=0.191\pm0.009$ and $T_N=14.5\pm0.2$. The evaluated β for $BaCoO_3$ also ranges between the predictions for the 2D and 3D Ising model ($\beta=0.125$ and 0.3125), and is roughly the same as that for $Ca_3Co_2O_6$ ($\beta=0.18\pm0.12$). This indicates a strong 2D character of the AF transition in $BaCoO_3$, in contrast to $\beta=0.31$ for the 1D antiferromagnet $CsCoBr_3$.[40] Here β of $CsCoBr_3$ was evaluated using the neutron diffraction data in the vicinity of T_N [$5\times10^{-4} \leqslant (T_N-T)/T_N \leqslant 0.08$], whereas β of $BaCoO_3$ uses the μSR data at $0.03 \leqslant (T_N-T)/T_N \leqslant 0.9$. According to Ref. 40, however, β of $CsCoBr_3$ looks almost the same value (0.31) even using the data at $0.03 \leqslant (T_N-T)/T_N$. The result that $\beta[BaCoO_3] < \beta[CsCoBr_3]$ is therefore reliable. This discrepancy is probably due to the difference of the d orbitals contributing to the magnetism; that is, t_{2g} for Co^{4+} in $BaCoO_3$ and t_{2g} and e_g for Co^{2+} in $CsCoBr_3$. The overlap of the former between the neighboring chains is expected to be smaller than that of the latter.[41]

The simple hexagonal structure of $BaCoO_3$ (and the lack of structural phase transitions at low T) and good quality of our sample suggest the difficulty for explaining five frequencies by multimuon sites and/or inhomogeneity of the sample. In addition the fact that the five frequencies show a sharp transition at the same temperature indicates that these are the intrinsic behavior in $BaCoO_3$. We consider the following two hypotheses.

(i) Coexistence of the 2D AF and 1D F interaction: According to the χ measurement at high T, the paramagnetic Curie temperature Θ_p was found to be ~22 K (consistent with the past work, $\Theta_p=17$ K).[22] This indicates that the magnitude of the interchain 2D AF interaction is roughly equivalent to that of the intrachain 1D F interaction, whereas the

former is less than the latter. The highest frequency in Fig. 10 (14.4 MHz) is comparable to the AF oscillation frequency in $Ca_3Co_2O_6$ (15 MHz at 1.8 K). The signals with ~5 MHz would correspond to the magnetic fields of the intrachain 1D F order.

(ii) AF domain structure: One CoO_3 chain [at (0,0)] is surrounded by six nearest-neighbor CoO_3 chains in the 2D-triangular lattice [see Fig. 2(c)]. We ignore the effect of the second nearest-neighbor chains. If the dipole field from the nearest-neighbor chain is defined as h at (0,0), the total field at (0,0) can be represented by $H_0, H_0 \pm 2h, H_0 \pm 4h$, and $H_0 \pm 6h$, in which H_0 is the field from the chain at (0,0). This could be consistent with a roughly symmetrical distribution of $\nu_{\mu,i}$ at 1.8 K [see Fig. 10(b)]. In this case, $\gamma_\mu/2\pi \times H_0 \sim 10$ MHz, where $\gamma_\mu/2\pi = 18.553\,42$ kHz/Oe. Furthermore, the electronic structural calculation suggested almost a similar stability for the two type of AF configuration, although the F configuration was predicted to be most stable.[24]

In order to further understand the nature of the AF phase in $BaCoO_3$, more precise μ^+SR measurements on pure and doped $BaCoO_3$ are necessary; in particular, the change in the interchain distance by chemical and/or physical pressure is crucial to distinguish the two hypotheses above through the shift of the balance between the 1D F and 2D AF interactions.

V. SUMMARY

Magnetism of quasi-one-dimensional (1D) cobalt oxides $A_{n+2}Co_{n+1}O_{3n+3}$ (A=Ca, Sr, and Ba, n=1, 2, 3, 5, and ∞) was investigated by susceptibility (χ) and muon spin rotation and relaxation (μ^+SR) measurements using polycrystalline samples at temperatures from 300 K down to 1.8 K. The χ measurement confirmed a systematic change in the charge and spin distribution in the 1D CoO_3 chain with n. The weak transverse field (wTF-)μ^+SR experiments showed the existence of a magnetic transition in all five samples investigated. The onset temperature of the transition (T_c^{on}) was found to decrease with n; that is, 100 ± 25 K, 90 ± 10 K, 85 ± 10 K, 50 ± 10 K, and 15 ± 1 K for n=1, 2, 3, 5, and ∞, respectively. In particular, for the samples with n=2–5, T_c^{on} was detected only by the present μ^+SR measurements. A muon spin oscillation was clearly observed in both $Ca_3Co_2O_6$ (n=1) and $BaCoO_3$ ($n=\infty$), whereas only a fast relaxation is apparent even at 1.8 K in the other three samples (n=2, 3, and 5).

A large negative paramagnetic Curie temperature for the samples with n=2 and 3 indicated that the transition at T_c^{on} is caused by an interchain two-dimensional (2D) antiferromagnetic (AF) interaction. Considering the structural similarity among the quasi-1D cobalt oxides, the transitions at T_c^{on} for the samples with n=1 and 5 were therefore most likely due to the appearance of the short-range 2D AF order. This suggested that the 1D ferromagnetic order in the CoO_3 chain of $Ca_3Co_2O_6$ (n=1) would occur at higher temperatures (~200 K) than proposed previously (~80 K).

For $BaCoO_3$ ($n=\infty$), the χ measurement confirmed that $T_c^{on} = T_N$(=15 K) and T_C=53 K, which corresponds to the ferromagnetic (F) transition caused by an intrachain 1D interaction. Nevertheless, the wTF-asymmetry (A_{TF}) did not exhibit a marked anomaly at T_C, while A_{TF} is very sensitive to the formation of magnetic order. This is likely to be caused by a domain motion in the 1D chain, as in the case for $CsCoCl_3$. In spite of the fact that the sample is structurally homogeneous, the ZF-μ^+SR spectrum showed a complex of at least five frequency components below T_N, which require further detailed studies.

ACKNOWLEDGMENTS

We thank Dr. S.R. Kreitzman, Dr. B. Hitti, and Dr. D.J. Arseneau of TRIUMF for help with the μ^+SR experiments. We appreciate useful discussions with Dr. R. Asahi of Toyota CRDL. This work was supported at Toyota CRDL by joint research and development with International Center for Environmental Technology Transfer in 2002–2004, commissioned by the Ministry of Economy, Trade, and Industry of Japan, at UBC by the Canadian Institute for Advanced Research, the Natural Science and Engineering Research Council of Canada, at TRIUMF by the National Research Council of Canada, and at Nagoya University (T. T.) by a Grant-in-Aid for the 21st Century COE program, "Frontiers of Computational Science."

*Corresponding author. Electronic address: e0589@mosk.tytlabs.co.jp

[1] J. Sugiyama, H. Itahara, T. Tani, J. H. Brewer, and E. J. Ansaldo, Phys. Rev. B **66**, 134413 (2002).

[2] J. Sugiyama, H. Itahara, J. H. Brewer, E. J. Ansaldo, T. Motohashi, M. Karppinen, and H. Yamauchi, Phys. Rev. B **67**, 214420 (2003).

[3] J. Sugiyama, J. H. Brewer, E. J. Ansaldo, H. Itahara, K. Dohmae, Y. Seno, C. Xia, and T. Tani, Phys. Rev. B **68**, 134423 (2003).

[4] J. Sugiyama, J. H. Brewer, E. J. Ansaldo, H. Itahara, T. Tani, M. Mikami, Y. Mori, T. Sasaki, S. Hébert, and A. Maignan, Phys. Rev. Lett. **92**, 17602 (2004).

[5] J. Sugiyama, J. H. Brewer, E. J. Ansaldo, B. Hitti, M. Mikami, Y. Mori, and T. Sasaki, Phys. Rev. B **69**, 214423 (2004).

[6] S. P. Bayrakci, C. Bernhard, D. P. Chen, B. Keimer, R. K. Kremer, P. Lemmens, C. T. Lin, C. Niedermayer, and J. Strempfer, Phys. Rev. B **69**, 100410(R) (2004).

[7] A. T. Boothroyd, R. Coldea, D. A. Tennant, D. Prabhakaran, L. M. Helme, and C. D. Frost, Phys. Rev. Lett. **92**, 197201 (2004).

[8] K. Boulahya, M. Parras, and J. M. González-Calbet, J. Solid State Chem. **142**, 419 (1999).

[9] M.-H. Wangbo, H.-J. Koo, K.-S. Lee, O. Gourdon, M. Evain, S. Jobic, and R. Brec, J. Solid State Chem. **160**, 239 (2001).

[10] H. Fjellvåg, E. Gulbrandsen, S. Aasland, A. Olsen, and B. C.

Hauback, J. Solid State Chem. **124**, 190 (1996).
[11] S. Aasland, H. Fjellvåg, and B. Hauback, Solid State Commun. **101**, 187 (1997).
[12] H. Kageyama, K. Yoshimura, K. Kosuge, H. Mitamura, and T. Goto, J. Phys. Soc. Jpn. **66**, 1607 (1997).
[13] H. Kageyama, K. Yoshimura, K. Kosuge, M. Azuma, M. Takano, H. Mitamura, and T. Goto, J. Phys. Soc. Jpn. **66**, 3996 (1997).
[14] B. Raquet, M. N. Baibich, J. M. Broto, H. Rakoto, S. Lambert, and A. Maignan, Phys. Rev. B **65**, 104442 (2002).
[15] B. Martínez, V. Laukhin, M. Hernando, J. Fontcuberta, M. Parras, and J. M. González-Calbet, Phys. Rev. B **64**, 12417 (2001).
[16] S. Rayaprol, K. Sengupta, and E. V. Sampathkumaran, J. Solid State Chem. **128**, 79 (2003).
[17] D. Flahaut, A. Maignan, S. Hébert, C. Martin, R. Retoux, and V. Hardy, Phys. Rev. B **70**, 94418 (2004).
[18] R. Fresard, C. Laschinger, T. Kopp, and V. Eyert, Phys. Rev. B **69**, 140405(R) (2004).
[19] E. V. Sampathkumaran, N. Fujiwara, S. Rayaprol, P. K. Madhu, and Y. Uwatoko, Phys. Rev. B **70**, 14437 (2004).
[20] V. Hardy, S. Lambert, M. R. Lees, and D. M. Paul, Phys. Rev. B **68**, 14424 (2003).
[21] Y. Takeda, J. Solid State Chem. **15**, 40 (1975).
[22] K. Yamaura, H. W. Zandbergen, K. Abe, and R. J. Cava, J. Solid State Chem. **146**, 96 (1999).
[23] K. Yamaura and R. J. Cava, Solid State Commun. **115**, 301 (2000).
[24] V. Pardo, P. Blaha, M. Iglesias, K. Schwarz, D. Baldomir, and J. E. Arias, Phys. Rev. B **70**, 144422 (2004).
[25] T. Li, G. D. Stucky, and G. L. McPherson, Acta Crystallogr. **29**, 1330 (1973).
[26] R. A. Gardner, M. Vlasse, and A. Wold, Acta Crystallogr. **25**, 781 (1969).
[27] N. Achiwa, J. Phys. Soc. Jpn. **27**, 561 (1969).
[28] G. Mihály, I. Kézsmárki, F. Zámborszky, M. Miljak, K. Penc, P. Fazekas, H. Berger, and L. Forró, Phys. Rev. B **61**, R7831 (2000).
[29] T. Inami, K. Ohwada, H. Kimura, M. Watanabe, Y. Noda, H. Nakamura, T. Yamasaki, M. Shiga, N. Ikeda, and Y. Murakami, Phys. Rev. B **66**, 073108 (2002).
[30] W. Higemoto, A. Koda, G. Maruta, K. Nishiyama, H. Nakamura, S. Giri, and M. Shiga, J. Phys. Soc. Jpn. **71**, 2361 (2002).
[31] T. Takami, H. Ikuta, and U. Mizutani, Jpn. J. Appl. Phys., Part 1 **43**, 8208 (2004).
[32] G. M. Kalvius, D. R. Noakes, and O. Hartmann, in *Handbook on the Physics and Chemistry of Rare Earths*, edited by K. A. Gschneidner, Jr. *et al.* (North-Holland, Amsterdam, 2001), Vol. 32, pp. 55–451, and references cited therein.
[33] This is consistent with the preliminary μ^+SR experiment on $Ca_3Co_2O_6$ using a pulsed muon beam at KEK [T. Takeshita, N. Nomura, K. Sato, S. Kaneko, T. Goto, J. Arai, K. Nishiyama, and K. Nagamine, in *The Abstracts of the Annual Meeting of the Physical Society of Japan 2003*, (unpublished), 22aTC-11, in Japanese]. However, there were neither information on A_{AF} and A_{fast} nor muon oscillation below T_N in the report, because of a limited time resolution of the pulsed beam (below ~10 MHz).
[34] H. E. Stanley, in *Introduction to Phase Transitions and Critical Phenomena* (Clarendon, Oxford, UK, 1971).
[35] N. Y. Vasanthacharya, P. Ganguly, J. B. Goodenough, and C. N. R. Rao, J. Phys. C **17**, 2745 (1984).
[36] H. Kageyama, K. Yoshimura, K. Kosuge, H. Nojiri, K. Owari, and M. Motokawa, Phys. Rev. B **58**, 11150 (1998).
[37] H. Yoshizawa, K. Hirakawa, S. K. Satija, and G. Shirane, Phys. Rev. B **23**, 2298 (1981).
[38] M. Mekata, S. Onoe, H. Kuriyama, B. J. Sternlieg, Y. Uemura, and K. Nagamine,J. Magn. Magn. Mater. **104**, 825 (1992).
[39] T. Takami, H. Ikuta, and U. Mizutani (unpublished).
[40] W. B. Yelon, D. E. Cox, and M. Eibschütz, Phys. Rev. B **12**, 5007 (1975).
[41] X. Jiang and G. Y. Guo, Phys. Rev. B **70**, 035110 (2004).